Experimental Research on Static Stiffness of the Planetary Roller Screw Mechanism

Shangjun Ma*, *Guanyu* Wu, *Jianxin* Zhang, and *Geng* Liu

Shaanxi Engineering Laboratory for Transmissions and Controls, Northwestern Polytechnical University, Xi'an, 710072, China

Abstract. This paper investigates the static stiffness characteristics of the planetary roller screw mechanism (PRSM). Firstly, an analytical model of elastic deformation in the PRSM considering contact deformation, combined deformation of screw shaft and thread deformations is established. Then, an accuracy coefficient is introduced to take into account the effect of machining error and assembly error on elastic deformation. Secondly, the stiffness tests of the PRSM are performed under different loads and nut positions. Lastly, the correctness of the analytical results is verified via the comparison with experimental results. The results show that the analytical results are in good agreement with the experimental results, and the stiffness variations under different loads and nut positions are obtained.

1 Introduction

Planetary roller screw (PRSM) is a mechanical transmission device, which can realize transformation of linear motion and rotary motion. As shown in Fig. 1, a PRSM primarily consists of a nut, screw and group of rollers, and it provides more contact points than conventional ball screw mechanisms (BSM) at a specific lead length. The advantages of the PRSM are high stiffness, high load capacity and compact structure, etc. Therefore, the PRSM has been increasingly used in engineering for motion and position control.

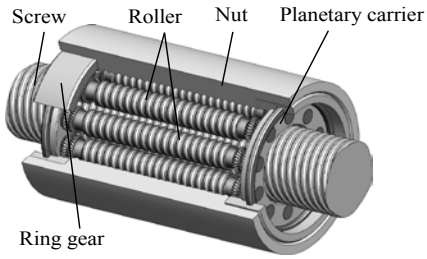

Fig. 1. The structures of the PRSM.

Earlier works on stiffness characteristics of the PRSM have included research on a calculation method for the static stiffness of PRSM [1-2]. In recent years, Jones [3] used a direct stiffness method to construct a stiffness model of the roller screw mechanism. In addition to predicting the overall stiffness of the mechanism, the distributions of the load across the threads of the individual bodies are also calculated. Yang et al. [4] used the roller as an object and investigated the load distribution and static rigidity of the PRSM. Morozov et al. [5] proposed a method for increasing the load capacity and rigidity of the PRSM by adjusting the screw surfaces. Abevi et al. [6] proposed an original approach based on the discrete model to calculate the static load distribution and the axial stiffness of the inverted PRSM. However, there are few experimental validations in the above models to support its engineering application. Also, the effects of machining error and assembly error on elastic deformation are not addressed.

Therefore, this paper provides an experimental research of the axial stiffness of the PRSM. Firstly, in section 2, the elastic deformation is studied, to obtain more accurate analytical results, an accuracy factor is introduced to revise the total deformation. Then, in section 3, the elastic deformation tests and axial stiffness calculations under different loads and different nut positions are further performed. Finally, the correctness of the analytical results is verified via the comparison with experimental results, and the variation trends between the loads and the stiffnesses are revealed.

2 Elastic deformations of the PRSM

2.1. Definition of axial stiffness

The axial stiffness of the PRSM can be defined as the ratio of axial load to deformation, which can be expressed as:

$$k = \triangle F/\triangle l \tag{1}$$

where k is axial stiffness of the PRSM, $\triangle F$ is axial load and $\triangle l$ is deformation under load $\triangle F$.

2.2. Elastic deformations of the PRSM

* Corresponding author: mashangjun@nwpu.edu.cn

In this paper, three kinds of elastic deformation such as contact deformation, combined deformation of screw shaft and thread deformations are considered.

2.2.1 Contact deformation

The contact deformation calculated by Hertzian contact theory is easily derived as [7]:

$$\delta_H = (9P_N^2/16E^2R_e)^{1/3}F_2(e) \quad (2)$$

where R_e is the equivalent radius, P_N is the normal load, E is the equivalent elastic modulus. $F_2(e)$ can be expressed as:

$$F_2(e) = 2/\pi(b/a)^{1/2}[F_1(e)]^{1/3}K(e) \quad (3)$$

$$F_1(e) = (4/\pi e^2)^{1/3}(b/a)^{1/2}\{[a^2/b^2K(e)\text{-}E(e)][K(e)\text{-}E(e)]\}^{1/6} \quad (4)$$

where e is the eccentricity of ellipse, and a and b are the semimajor axis and the semiminor axis of the contact ellipse, respectively. $K(e)$ and $E(e)$ are elliptic integrals of the first kind and second kind, respectively.

2.2.2 Combined deformation of screw shaft

The tension or pressure deformation, torsional deformation and bending deformation of screw shaft are considered in this section. The combined deformation is represented as [8]:

$$\delta_S = (4/E\pi d_s^2+8L_s^2/\pi^3 d_s^4\eta G)Fx+y\tan\alpha \quad (5)$$

where F is the working load, x is the working position of the nut and d_s is the nominal diameter of screw thread. G is shear modulus, L_s is the lead of the screw and η is the transmission efficiency. α is helix angle of the screw and y is the deflection caused by the weights of the screw shaft.

In Eq. (3), the first item in brackets on the right of the equal sign is tension or pressure deformation, the second item in brackets is torsional deformation and the last item is bending deformation.

2.2.3 Thread deformations

The thread deformations in the axial direction include deformations caused by bending σ_1, shear σ_2, thread root lean σ_3, thread root shear σ_4 and radial shrinkage (or radial expansion) σ_5.

The detailed calculation method can be found in references [9]. The total deformation of the screw thread σ_S, roller thread σ_R and nut thread σ_N can be written as:

$$\sigma_S = \sigma_1+\sigma_2+\sigma_3+\sigma_4+\sigma_{5S} \quad (6)$$

$$\sigma_R = \sigma_1+\sigma_2+\sigma_3+\sigma_4+\sigma_{5S} \quad (7)$$

$$\sigma_N = \sigma_1+\sigma_2+\sigma_3+\sigma_4+\sigma_{5N} \quad (8)$$

The total deformation of the thread in the axial direction is denoted as δ_T, resulting in:

$$\delta_T = \sigma_S+2\sigma_R+\sigma_N \quad (9)$$

The total deformation of the PRSM in the axial direction can be expressed as:

$$\delta_{PRSM} = \delta_H+\delta_T+\delta_S \quad (10)$$

2.3. Accuracy coefficient

In order to consider the effects of machining error and assembly error on elastic deformation on the load bearing region, an accuracy factor is introduced to revise the total deformation. According to the comparison research of stiffness between PRSM and BSM [2], the value of accuracy coefficient of the PRSM can refer to the value of BSM [10], as shown in Table 1.

Table 1. Accuracy coefficient of the PRSM.

Accuracy level	1	2	3	4	5
f_{ar}'	1.667	1.724	1.818	1.887	2

The total deformation of the PRSM considering accuracy coefficient in the axial direction can be rewritten as:

$$\delta'_{PRSM} = f_{ar}'(\delta_H+\delta_T)+\delta_S \quad (11)$$

3 Stiffness experiment

3.1. Experimental system

The test rig is shown in Fig. 1. In stiffness testing, two physical quantities need to be collected: axial load and axial displacement (axial elastic deformation). According to the definition of stiffness, the measuring principle of axial stiffness is that the screw is fixed and the rotation of the nut is limited, the axial load is applied on nut, and the displacement change of the nut relative to the screw under the action of axially loaded is measured. Therefore, the clamping sets are used to fix the screw and the anti-rotation device is designed to limit the rotation of nut. At the load end, the hydraulic cylinder is used as the power source to achieve axial loading, the linear grating ruler is used to detect the displacement of the nut relative to the screw.

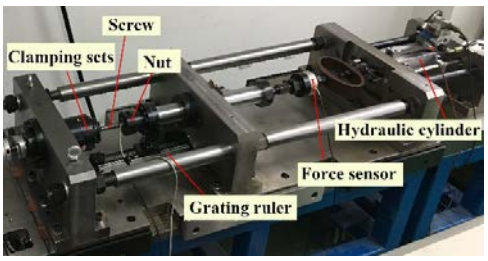

Fig. 2. The test rig of axial stiffness.

3.2. Experimental results

Force-deformation curves are obtained under different nut positions (The distance l_{Nut} between the nut and the fixed end of the screw is used to denote the nut position), as shown in Figs. 3-5. The accuracy coefficient is 1.818.

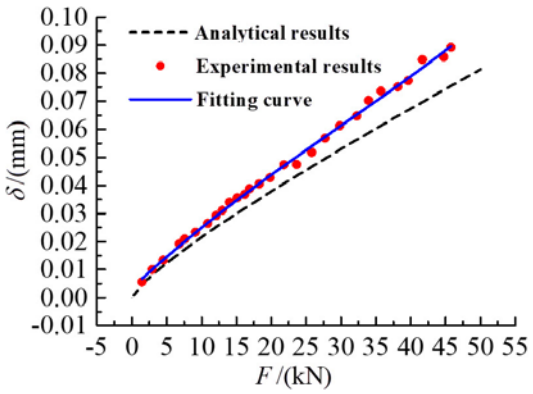

Fig. 3. l_{Nut}=60mm.

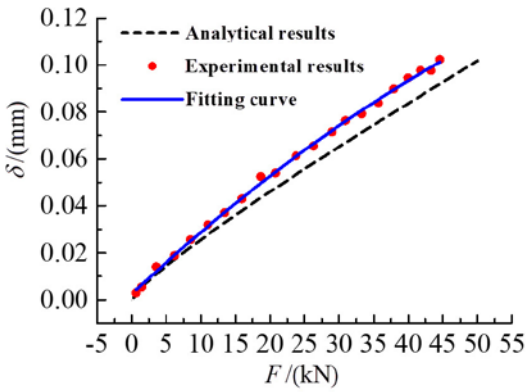

Fig. 4. l_{Nut}=92mm.

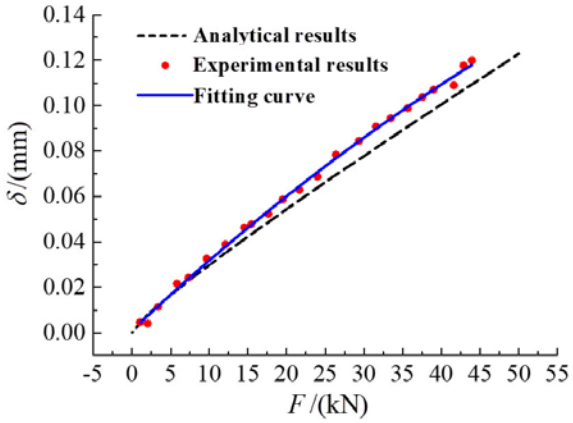

Fig. 5. l_{Nut}=125mm.

Figs. 3-5 show that the fitting curves of axial deformation are similar to that of theoretical curves. When the load is less than 10 kN, the difference is small. However, when the load is greater than 10 kN, the different increases with the increase of the load. The larger the distance l_{Nut}, the larger the deformation, that is, the axial stiffness of the PRSM decreases with the increase of the distance l_{Nut}.

The possible reasons are as follows: 1) the deformation measured by experiment also contains other deformations such as the structural deformation of the test rig, the clearances of the sensors and the clearances of the components of PRSM [11-12]; 2) the accuracy coefficient is an empirical value, which requires a lot of experiments to obtain. In addition, the selection of accuracy coefficient in this paper refers to the BSM, and the axial stiffness of PRSM may be more sensitive to machining errors.

According to the data in the Figs. 3-5 and Eq. (1), the experimental and analytical results of the axial stiffness of PRSM under different loads and different nut positions can be calculated respectively, as shown in Tables 2-4.

Table 2. Comparison of experimental and analytical results of axial stiffness (l_{Nut}=60mm)

Load / Stiffness	10 kN	20 kN	30 kN	40 kN	46 kN
Experimental results (10^5N/mm)	4.6394	5.2817	5.6634	5.9345	6.0659
Analytical results (10^5N/mm)	4.0236	4.6424	4.9286	5.1285	5.2115
Relative error	13.27%	12.10%	12.97%	13.58%	14.09%

Table 3. Comparison of experimental and analytical results of axial stiffness (l_{Nut}=92mm).

Load / Stiffness	10 kN	20 kN	30 kN	40 kN	46 kN
Experimental results (10^5N/mm)	3.9063	4.3478	4.6012	4.7790	4.8352
Analytical results (10^5N/mm)	3.4087	3.8499	4.0553	4.2298	4.3518
Relative error	12.74%	11.45%	11.86%	11.49%	9.99%

Table 4. Comparison of experimental and analytical results of axial stiffness (l_{Nut}=125mm).

Load / Stiffness	10 kN	20 kN	30 kN	40 kN	46 kN

Load / Stiffness	10 kN	20 kN	30 kN	40 kN	46 kN
Experimental results (10^5N/mm)	3.3520	3.6749	3.8557	3.9795	4.0196
Analytical results (10^5N/mm)	2.9933	3.3650	3.4810	3.6477	3.6681
Relative error	10.70%	8.43%	9.72%	8.34%	8.74%

As shown in the tables above, the relative error between the experimental and analytical results is between 8% and 15%, and the relative error of the axial stiffness decreases with the increase of the distance between the nut and the fixed end of the screw. This is because the deformation on the load bearing region is affected by the machining accuracy. With the increase of the distance between the nut and the fixed end of the screw, the proportion of the deformation on the load bearing region in the overall deformation decreases continuously, which further leads to the decrease of the relative error. Therefore, to improve the static stiffness characteristic of the PRSM, the thread thickness should be increased appropriately, and the auxiliary support should also be increased when the nut stroke is longer.

4 Conclusions

This study develops an analytical model to investigate the static stiffness characteristics of a PRSM based on the Hertz contact theory. The experimental research under different loads and nut positions was performed to verify the correctness of the analytical model. The relative error between the experimental and analytical results is between 8% and 15%, which is acceptable. The results can be used to guide the parameter design and help improve the transmission quality. Planned future research will focus on a large number of experiments to obtain more accurate accuracy coefficients and identifying the influencing factors of deformation in the test rig.

The research is supported by National Natural Science Foundation of China (Grant No. 51875458), Key Project of National Natural Science Foundation of China (Grant No. 51535009) and the Fundamental Research Funds for the Central Universities (Grant No. 31020190504003).

References

1. J. Otsuka, T. Osawa, S. Fukada, A study on the planetary roller screw, comparison of static stiffness and vibration characteristics with those of the ball screw, Bull. Jpn. Soc. Precis. Eng. **23**, 3 217-223 (1989)
2. Q.Z. Jin, J.J. Yang, J.L. Sun, The comparative research on the static stiffness of ball screw and planetary roller screw, J. Mech. Sci. Technol. **18**, 2 230-232 (1999)
3. M.H. Jones, S.A. Velinsky, Stiffness of the roller screw mechanism by the direct method, Mech. Based Des. Struct. Mach. **42**, 1 17-34 (2014)
4. J.J. Yang, Z.X. Wei, J.S. Zhu, W. Du, Calculation of load distribution of planetary roller screws and static rigidity, Huazhong Univ. Sci. Technol. **39**, 4 1-4 (2011) (in chinese)
5. V.V. Morozov, V.I. Panyukhin, A.V. Zhdanov, Increasing the load capacity and rigidity of roller-screw mechanisms by adjusting the screw surfaces, Vestn. Mashinostr. **2** 15-21 (2016)
6. F. Abevi, A. Daidie, M. Chaussumier, M. Sartor. Static load distribution and axial stiffness in a planetary roller screw mechanism, J. Mech. Des. **138** 1 012301-8 (2011)
7. K.L. Johnson, *Contact Mechanics* (Cambridge University Press, ISBN: 0521347963, 1987)
8. S.J. Ma, W. Cai, L.P. Wu, G. Liu, P. Cheng, Modelling of transmission accuracy of a planetary roller screw mechanism considering errors and elastic deformations, Mech. Mach. Theory. **134** 151-168 (2019)
9. W.J. Zhang, G. Liu, R.T. Tong, S.J. Ma. Load distribution of planetary roller screw mechanism and its improvement approach, Proc. Inst. Mech. Eng. Part C-J. Eng. Mech. Eng. Sci. **203-210** 1989-1996 (2015)
10. Ball screw mechanism, Part four: Axial static stiffness, (Standards Press of China, GB/T17587.4-2008, Beijing, 2008)
11. S.J. Ma, L.P. Wu, X.J. Fu, Y.J. Li, G. Liu. Modelling of static contact with friction of threaded surfaces in a planetary roller screw mechanism, Mech. Mach. Theory. **139** 212-236 (2019)
12. S.J. Ma, L.P. Wu, G. Liu, X.J. Fu. Local contact characteristics of threaded surfaces in a planetary roller screw mechanism, Mech. Based Des. Struct. Mach, Online Doi: 10.1080/15397734. 2019. 16159 44 (2019)